Manuscript Submitted	26.6.2024
Accepted	21.11.2024
Published	3.6.2025

Automatic Weld Bead Discontinuities Detection based on Dye Penetrant Test by Deep Learning

Saipul Azmi Mohd Hashim, Nor Mohd Syamsi Abd Malek,
Mohanadhas Kanagaraj, Mohd Faizal Yasak
Manufacturing Technology Unit
Kolej Komuniti Kepala Batas, Kolej Komuniti Kuantan, Kolej Komuniti Taiping
saipulneural@gmail.com, syamsimalek@gmail.com, mohanadhas@kkkba.edu.my, fyasak@gmail.com

Abstract

Dye Penetrant Test is widely used in manufacturing industries, solely inspected by human eyes. The test using the human eye to detect the dye trap in weld surface cavity discontinuities – crack and porosity. However, the test is prone to the human factor effects and this led to erroneous results, hence automation is desired. This paper aims to propose a system by Deep Learning approach using SqueezeNet Framework based on the test. A dataset was obtained from a set of weld bead soft steel plates welded by arc welding process covering 258 RGB digital images in three categories – normal, crack, and porosity. The result through the proposed system is excellent by 100% precision, 87.5% recall, and 92% accuracy. Besides, it is statically good with F-score at 93.33% and found statistically significant. This result is uplifting, hence by this data the proposed system is acceptable to replace human inspection.

Keywords: *Welding, Deep Learning, SqueezeNet Model, Die Penetrant Test.*

1. INTRODUCTION

High level of parts violation may be the main reason of catastrophes and accidents occurs in production line (Glebov & Lashmanov, 2015). By number of reasons, while the part is used in production line, minor discontinuity occurs on the part and the discontinuity enlarges before it hit total breakdown. Hence, part that is installed in production lines need for a test to detect the discontinuity occurrence. Furthermore, the test is required to not to destruct the part as this is not economic for the production cost. Therefore, for this reason a Non-destructive Test (NDT) such as Dye Penetrant Test (DPT) is an efficient tool to find the discontinuity timely and early correction can be taken to prevent the discontinuity enlarge into total breakdown. This is due to the flexibility use of the test as it is applicable in in-process, final, and maintenance examinations (ASTM E165/E165M-23, 2023).

In practice, part of the DPT is inspected by an authorized inspector's human eye. Generally, the inspector's standard operation begins with surface cleaning, followed by a penetrant liquid application – by either dripping, spray, or brushing, then excess penetrant removal, application developer, inspection test by human eye, and ends up with weld bead surface cleaning (Dwivedi, 2022). The advantage of DPT is, it can be done on site as it is portable, plus it needs no additional resources such as electricity and water. Furthermore, with special dye material use, the test can detect to the smallest crack size up to $0.03 - 0.05$ inch length of the crack (Koshti, 2018).

Although DPT is not a sophisticated test, it is used extensively in the aerospace (Shipway et al., 2021), automotive, rail, petrochemical, and machinery industries (Karatay et al., 2017). DPT in manufacturing industry commonly used in casting, forging, and welding operation to locate surface discontinuities such as laps, seams, cracks, and porosity. In welding works, a poor bead profile reduces the joint's mechanical properties, shorten the product lifetime, and even turned a structure to break down

(Rodríguez-Gonzálvez et al., 2017). The poor weld bead profile is defined as weld surface discontinuities. These surface discontinuities include porosity, surface crack, burn through, under fill, poor penetration, undercut, and spatter. Based on these, porosity and surface crack are this study interest discontinuities. Besides, these two are the main cause of welding failure, due to the porosity reduces the strength and fails a structure due to fatigue, and the surface crack fails and propagates crater crack (Dwivedi, 2022). Basically, the use of DPT of a welded plate is to visualize clearly the full length of any discontinuities that appear at the weld bead surface. This dye enters into a discontinuity cavity by capillary action, then the remaining dye on the surface is removed and the left dye has embedded itself in the discontinuities cavity (Eisenmann, 2018). By DPT, the dye colour is a significantly contrast to the part body colour and the test produced indications are much broader than the actual discontinuities, hence these causes the discontinuity visible easily.

However, due to the discontinuity detection by DPT inspection is solely by human eye, hence it leads to the test variable results. This makes the inspection is error prone and lessen the defect detection rate due to the variation of background noise, the presence of large defects, and human visual fatigue cause by inspecting large number of parts (Charles et al., 2015). Therefore, automation of detecting the discontinuity is desirable (Shipway et al., 2021; Gültekïn et al., 2019) to detect discontinuities early and preventing production line catastrophes and accident's occurrence. Besides, based on previous literature in this study line, the automation improved the result reliability (Shipway, 2019), and more sensitive quality inspection (Gültekïn et al., 2019). The advantage is the automated system, it increased the test speed and the test accuracy in detecting defects on the surface (Endramawan & Sifa, 2018), plus the automated test is simple and cost effective (Karatay et al., 2017) compare to the test applied manually. Due to the previous research success, the expectation is this study feasible and reliable.

It is anticipated, the existence of current technology that is suitable to replicate DPT and herewith the technology used in this paper is based on Artificial Intelligence (AI) to read digital images. In addition, the technology classifies images by normal and detected discontinuities. Besides, in this paper, the technology is Deep Learning (DL), one of the AI approaches, used to automate the image classification. DL is selected for this paper due to the approach is the current trend for image classification, and it is extensively used in the replication of Non-Destructive Tests (Shipway et al., 2021) which include various visual inspection tests. Moreover, DL is proven to automatically extract meaningful feature in raw data, surpasses human performance in analysis and forecasting data (Loukil et al., 2023). It is a useful technique to almost every application field, learns the features as the input and mapping of the output automatically, and applicable with different dataset types such as images, signal, and numerical data (Sharma et al., 2021). These facts back the use of DL approach in this study.

Quality assurance mainly in manufacturing industry NDT is intensively benefited by the use of DL (Tercan & Meisen, 2022). DL has been highly recognised in the manufacturing industries and widely applied in NDT image-based techniques (Xu et al., 2022). For instance, Kong & Ni (2020) applied DL to find failure in wafer based on digital images in semiconductor manufacturing. Besides, DL applied for defect evaluation based on X-ray images in 3D printer making Aluminium Alloy product (Xu et al., 2024) and welding production (Yang et al., 2021). DL also used to replace manual visual inspections based on digital images to inspect damage in laminated composite structure (Fotouhi et al., 2021), metallic corrosion (Yu et al., 2023) and plastic bottle surface defect (Kazmi et al., 2023). This paper is aligned with these literatures and suggests it is in the current study trend.

Based on these facts and this paper interests, this paper aims to propose an automatic system to detect the surface discontinuity on weld bead based on DPT. The rest of the paper is organized as follow. Section 2 describes the methodology used to develop the system. Section 3 spells out the result and analysis. This paper's conclusion and future suggestion is to wrap in Section 4.

2. METHODOLOGY

2.1 Data Acquisition

Digital images are obtained from the actual exercise of DPT in production line of welding work. The images captured by 16MP camera on weld bead of soft steel plates welded with an arc welding process. These images can be categorised into good weld bead profile or normal, surface crack, and porosity about the bead. To simplify the following terms are used for the category is normal, crack, and porosity. In addition, the use of MATLAB version R2020a, for the DL system development and data analysis, it requires certain image setup. The software also accepted RGB format images, and applied in this study. Besides, the software supports the image size up to the maximum of 4.6MB and image pixel size is 227-by-227. Image study samples are shown in Figure 1, and there are 258 images are applied – 92 normal images, 82 crack images, and 84 porosity images are the image category number.

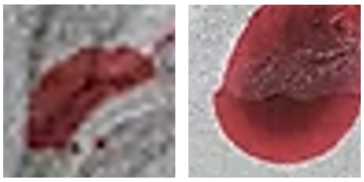

(a) Crack Image Samples

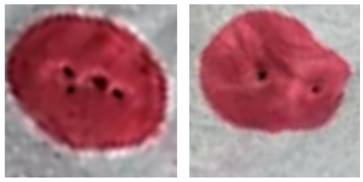

(b) Porosity Image Samples

Figure 1: Sample of RGB format images for the Crack and Porosity resulted by DPT

2.2 Deep Learning

DL higher accuracy in automating image classification superseded other approaches and widely used in researches and applications (Bhole & Kumar, 2020; Sethy et al., 2020). Besides, because of the DL excellent performance in image classification it is the current trend AI approach in this study line (Elkorany & Elsharkawy, 2021). By this advantage, DL is applied in this study, is derived from Convolutional Neural Network (CNN) (Li et al., 2021), and is inspired by the normal technique of organisms' visible conception (Obaid et al., 2022). This make it works is logically acceptable in manipulating digital image application. In addition, this network is proven successfully applied to solve many challenging computer vision tasks such as object classification and target detection (Fu et al., 2019). This network is believed feasible in solving the aforementioned problem – classification by detecting normal, crack, and porosity images. Hence, these facts and claims justified the approach use.

Developing a network's framework consuming a lot of time and repetitive works to develop an efficient framework. In designing DL, there are two option approaches of developing and training a framework – (i) Training from scratch, (ii) Adjusting a Pre-Trained Framework (Bhole & Kumar, 2020). Due to training from scratch required too much time, thus this study prefers to apply the second approach, i.e. Adjusting a Pre-Trained Network -- also known as Transfer Learning (TL). Though, through TL much work in developing a framework from scratch is reduced or bypassed, work of applying the TL framework for a new data still requires much work. As it is named, a Pre-Trained Network is designed by previous researcher where it is proven effective in classifying data. In addition, the TL refers to a designed framework that need for new weights to set the pattern of a new data. Thus, new framework training is required. Due to this is the proven an effective trained framework, therefore it is expected to be effective and can be reused onto other new data. The framework usage required work as follows: selecting a framework model, modifying, fitting, and retraining (Bhole & Kumar, 2020), so that it will works with the new data. Furthermore, due to the framework is well developed, hence it required much smaller data and computational time lesser to be re-trained onto a new data, compare to a new framework developed from scratch (Bhole & Kumar, 2020). Beale, Hagan, and Demuth (2020) list down a number of TL framework can be used such as Xception, Darknet-19, ResNet-50, and SqueezeNet. SqueezeNet is the selected framework for this image classification study. Through literature study, based on our knowledge, there are two previous studies that is much closed this paper. The researchers replicated DPT uses DL for the image classification based on self-develop framework (Karigiannis et al., 2021), and ResNet34 and RestNet50 framework (Shipway et al., 2021).

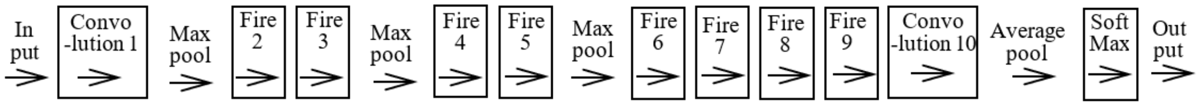

Figure 2: SqueezeNet framework

SqueezeNet framework consists of two convolution layers, i.e. Convolution 1 and Convolution 10, eight fire module layers (fire2-fire9), three max pooling layers, one global average pooling layer and the last one is softmax layer (Elkorany & Elsharkawy, 2021). This framework is visualised in Figure 2. The first layer, i.e. Convolution 1 filters the input that generates the activation of the model influences detecting feature in an input. This layer resulted a filter is developed once the input is multiplied within a set of weights which resulted two-dimensional filter for an input. This two dimensional filter suitable for an image input (Li et al., 2021). They transformed image inputs with the interest to gather information whole image and not focusing on one point of location. For instance, in an image application, the filter applies across the image in order to detect a specific type of feature in it – the feature is designed in two dimensional location of the image. Operationally, this layer operates in two convolution layers – Convolution 1 and Convolution 2. The first layer squeezed the data into 1 x 1 convolutional filter and the second layer expands the data using 1 x 1 and 3 x 3 convolution filters (Ashhar et al., 2021). The purpose of squeeze the data to generate the input array multiple times at different points on the entire image area as the input. Thus, feature discovering is enabled from the entire digital image area. This layers' mechanism resulted an effective framework (Wang et al., 2023). Besides, though the parameter minimization has already initiated in the first convolution layer, the framework still needs additional eight fire modules in the SqueezeNet framework. They also reduce the input volume resulting in the parameter number minimization (Obaid et al., 2022). By applying these modules in a sequence of layers, they are progressively minimizing input parameters continuing with the second to the ninth fire module, hence only efficient of parameters is obtained. Moreover, in the pooling layers – two Max Pooling layers and an average pooling layer, are utilised to fasten the output generation (Guo et al., 2017). Following layer, a SoftMax activation function is applied to predict the score for each set output parameter. Finally, the convoluted output from the input is generated and gathered.

3. RESULT AND ANALYSIS

This study is based on the 258 images as the input for DL with SqueezeNet framework. Besides, three categories of weld bead conditions are gathered – normal, crack, and porosity. The total number images for normal is 92, crack is 82, and porosity is 84. These total number of images are set in following classes for the computational in the used software – 70% (180) for training, 20% (50) for testing, and 10% (28) for validating. In addition, these three image class selection is set at random.

3.1 Accuracy and Loss through the System's Framework Training

An epoch is a full training cycle on the entire data set (Beale et al., 2020). In learning process, it is a waste of time to apply as many epochs defaulted by the used software. Thus, setting the maximum number of epochs is required. Based on the setting of maximum epoch to 5, the training result is shown in Figure 3(a). Training result i.e. accuracy and loss can only measure after the training is runs, thus the result is beginning after the iteration 0 value. Besides, the iteration is stopped at epoch 5 as initially setup. In this context, accuracy refers to the rate of correct classification, and loss refers to the rate of incorrect classification. The chart is easily generated by the used software and it shows the based-on validation data. In addition, the chart shows while the accuracy graph is going uphill, the loss graph showing downhill. If the performance of the accuracy is poor, hence the data and other setting need to be reset, which retraining is required. However, for this case, the system performance shows good accuracy i.e. 92.86% -- two incorrect detection out of 28 validating data size. The two incorrect detections are in normal weld category image, that detected as porosity category image. Hence the framework reset and retraining is not required. This analysis involved data training and data validation, conversely the following subsection is based on testing data.

3.2 System Performance Evaluation

Initially, for fundamental analysis, common charts are introduced in this study – Confusion and Histogram charts. Confusion Chart indicates the categories that are being confused by the proposed system as other category in this case normal, crack, and porosity. The chart is easily generated by the software used and it shows how many detections are correct and incorrect per category, in summary of all detection done by the system. This chart shown in Figure 3 (b), vertical condition is the true category and horizontal condition is the predicted category. Based on this result, the following Figure 3 (c) Correct and Incorrect Rate Histogram chart is generated. For clarification, Figure 3(b) and 3(c) is based on testing data. This chart shows number and the percentage for each category performance. The correct rate for porosity is 24%, normal is 36%, and crack is 32%. Moreover, normal category incorrectly detected in 8%, and other category's incorrect rate at 0%.

Then, for accessing the framework defect detection by classification performance, the evaluation measurement is introduced in this subsection. Primarily, the data can be categorized by image correctly detected (P) and image incorrectly detected (N). Further categorized of the data that represents parameters in this study includes: the defect images correctly detected number known as True Positive (TP); True Negative (TN) stands for normal images detected as no-defect number; no-defect images incorrectly detected as defect number as False Positive (FP); and defect images incorrectly detected as no-defect number as False Negative (FN). Thus, based on these parameters, following are the measurement performance evaluation parameters are calculated used to measure the proposed system performance – Precision (Pr), Recall (Re), and Accuracy (ψ).

$$\mathrm{Pr} = \frac{TP}{TP + FP} \quad (1) \qquad \mathrm{Re} = \frac{TP}{TP + FN} \quad (2) \qquad \Psi = \frac{TP + TN}{P + N} \quad (3) \qquad \gamma = 2\frac{Pr \times Re}{Pr + Re} \quad (4)$$

Precision value measures the system's accuracy in detecting an image as positive or normal image. Recall is the term measures the system's ability to detect positive images. In addition, the value of accuracy is defined as the ratio between the correct detection of images in the total number of images. These values are well pictures classification performance in percentage. Based on the initial result, the value of P is 18, N is 32, TP is 28, TN is 18, FP is 0, and FN is 4. Thus, the value of Pr is 1 (100%), Re is 0.875 (87.5%), and Ψ is 0.92 (92%). These values are calculated based on equation (1), (2), and (3).

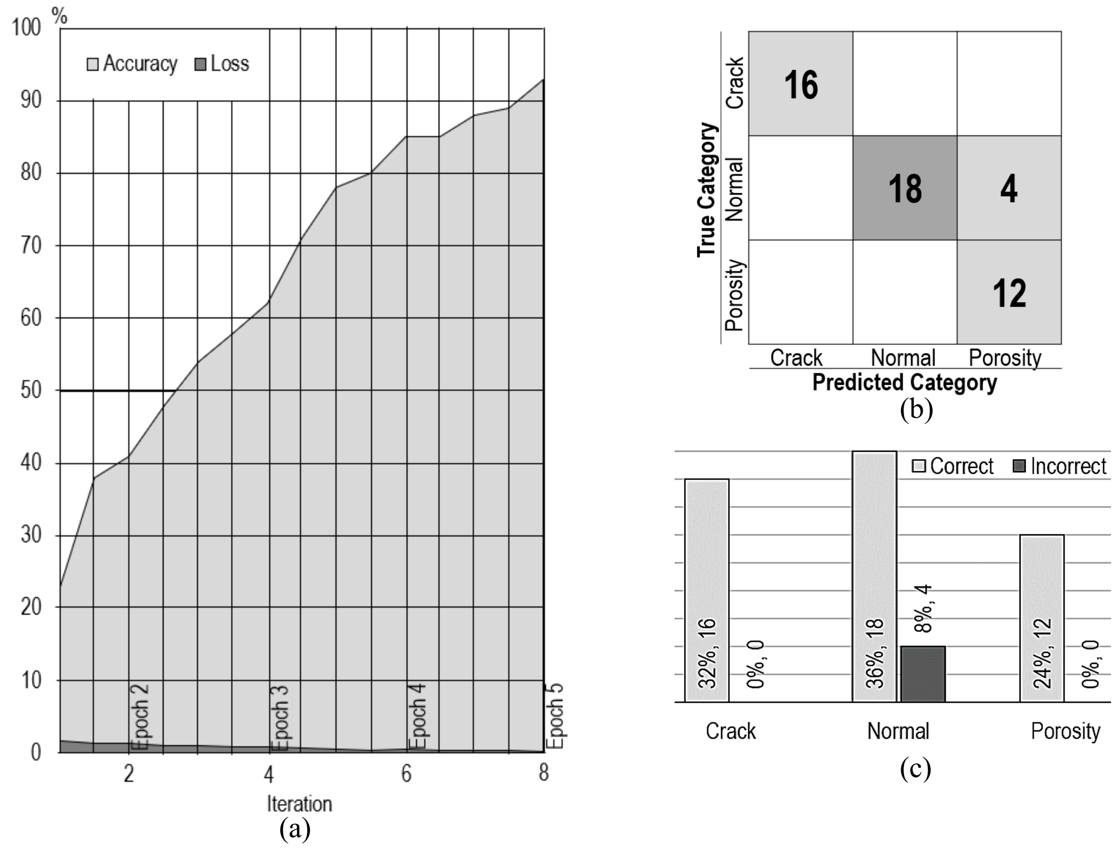

Figure 3: Result Analysis Charts – (a) Accuracy and Loss Chart; (b) Confusion Chart; (c) Correct and Incorrect Rate Histogram Chart.

3.3 Statistics Tests

Due to in this study, the detection performance can be measured on two sample sets, i.e. testing data and validation data, thus two options can be run for the statistical tests. The fact is, the minimum required sample size (n) for the statistical test is equal or above 30. Unfortunately, due to validation data n is below 30, hence the statistical tests are invalid to run on the sample. Therefore, the result based on testing data is used, with the data n of 50.

F-score (γ) as in equation (4) is a statistical parameter indicates the best performance achieved by a system. The logical highest value is 1.0, that representing ideal value for Pr and Re. The excellent contributions of the deep learning with SqueezeNet framework used in this study were clarified by this analysis that the obtained F-score is 93.33%. In addition, statistic testing is conducted with the data in this study to know the result margin of error. With the desired confidence level of 99% ($z^* = 2.58$), the calculated margin of error for the result obtained is plus and minus of 14.59%. Besides, by the result of classification rate for this study is 92%, the idea is to know the probability of this rate can be re-obtained by reshuffle the collected data. Statistically, this can be done by finding the value of confidence interval. By 95% desire confidence ($z^* = 1.96$), for the rate to be re-obtained, the confidence interval is between 91.08% and 68.92%. Moreover, the results' values that represent the population, recall (87.5%) and accuracy (92%) are tested by Hypothesis Test. By 95% confidence, the p-value for the recall is 0.0548 and accuracy is 0.0009. The p-value for recall is marginally significant, hence the value of 87.5% is accepted as it is null hypothesis (H_0) value. However, p-value for accuracy represent highly statistically significant, hence H_0 can be rejected. Thus, accuracy percentage probably can be higher than 92%.

4. CONCLUSION AND FUTURE RECOMMENDATION

In this paper, DL using SqueezeNet framework used to perform classification of defective welded part and acceptable welded part based on weld bead surface profile – crack, porosity, and normal. Based on the analysis, the first conclusion is that the system is an excellent classifier with high percentage of precision (100%), recall (87.5%), and accuracy (92%). Besides, for the second conclusion, statistically confirmed the system best performance can be achieved at high level – F-score is 93.33%. Therefore, this paper indicates the proposed system is an effective yet efficient to do classification tasks by replicating DPT operation. This study also concluded that though normal images can be efficiently detected but the chances it incorrectly classifies as porosity image is also high. The third conclusion suggests that the result by validation data agrees with the result by testing data. In other words, the collected data is consistently at the whole level. By statistical tests also the conclusion is the gathered results via this study is with high statistical confidence – non- bias nor the result is not by chance, it can be achieved repetitively.

For upcoming study, the proposed system is suggested to embed in a more general system that is applicable in realistic volume. Hence, more categories of images should be covered in the study. Moreover, for future study the system can be extended as a dynamic image system, e.g. video, since in manufacturing industry application, the inspection process involved the whole welded part or weld bead area. Furthermore, the suggestion is to apply other NDT tests in manufacturing facilities such as Visual Inspection, Radiographic Testing, and Ultrasonic Testing to widen the system performance and efficacy, and exploring the system's adoption for other manufacturing process system.

ACKNOWLEDGEMENT

This research was not funded by any grant.

REFERENCES

American Society for Testing and Materials. (August, 2023). *Standard Practice for Liquid Penetrant Testing for General Industry* (ASTM E165/E165M-23). ASTM International. https://www.astm.org

Ashhar, S. M., Mokri, S. S., Abd Rahni, A. A., Huddin, A. B., Zulkarnain, N., Azmi, N. A., & Mahaletchumy, T. (2021). Comparison of deep learning convolutional neural network (CNN) architectures for CT lung cancer classification. *International Journal of Advanced Technology and Engineering Exploration*, *8*(74), 126.

Beale, M. H., Hagan, M. T., & Demuth, H. B. (2020). Deep learning toolbox user's guide. *The Mathworks Inc.: Herborn, MA, USA*.

Bengio, Y. (2009). Learning deep architectures for AI. *Foundations and trends® in Machine Learning*, *2*(1), 1-127.

Charles, R. L., Johnson, T. L., & Fletcher, S. R. (2015). The use of job aids for visual inspection in manufacturing and maintenance. *Procedia CIRP*, *38*, 90-93.

Dwivedi, D. K. (2022). *Fundamentals of metal joining*. Springer Singapore.

Eisenmann, D. (2018). Liquid Penetrant Inspection. In Anderson, K., Weritz, J., & Kaufman, J. G. (Ed.). *ASM Handbook, Volume 2A: Aluminum Science and Technology* (pp. 46-59). *ASM International*.

Elkorany, A. S., & Elsharkawy, Z. F. (2021). COVIDetection-Net: A tailored COVID-19 detection from chest radiography images using deep learning. *Optik*, *231*, 166405.

Endramawan, T., & Sifa, A. (2018, February). Non-destructive test dye penetrant and ultrasonic on welding SMAW Butt joint with acceptance criteria ASME standard. In *IOP Conference Series: Materials Science and Engineering* (Vol. 306, No. 1, p. 012122). IOP Publishing.

Fotouhi, S., Pashmforoush, F., Bodaghi, M., & Fotouhi, M. (2021). Autonomous damage recognition in visual inspection of laminated composite structures using deep learning. *Composite Structures*, *268*, 113960.

Fu, Y., Sun, T., Jiang, X., Xu, K., & He, P. (2019, October). Robust GAN-face detection based on dual-channel CNN network. In *2019 12th International Congress on Image and Signal Processing, BioMedical Engineering and Informatics (CISP-BMEI)* (pp. 1-5). IEEE.

Glebov, V., & Lashmanov, O. U. (2015, June). Modelling of microcracks image treated with fluorescent dye. In *Modeling Aspects in Optical Metrology V* (Vol. 9526, pp. 316-321). SPIE.

Gültekïn, E., Çelik, H. İ., Dülger, L. C., Sünbül, H. İ., & Harun, K. A. N. İ. (2019). Image Processing Applications on Yarn Characteristics and Fault Inspection. *Tekstil ve Mühendis*, *26*(116), 340-345.

Guo, K., Sui, L., Qiu, J., Yu, J., Wang, J., Yao, S., Han, S., & Wang, H. (2017). Angel-eye: A complete design flow for mapping CNN onto embedded FPGA. *IEEE transactions on computer-aided design of integrated circuits and systems*, *37*(1), 35-47.

Karatay, M., FZ, B. M., Guldu, K., & Harmansah, C. (September 2-4, 2017). Investigation of Usability of Fluorescent and Radiolabeled Liquid Penetrant as a Non-Destructive Testing Agent. *The 14th International Conference of the Slovenian Society for Non-Destructive Testing*, Bernardin, Slovenia.

Karigiannis, J., Liu, S., Harel, S., Bian, X., Zhu, P., Xue, F., Bouchard, S., Cantin, D., Beaudoin-pouliot, M., Bewlay, B. P., & Caron, M. C. (2021). Multi-robot system for automated fluorescent penetrant indication inspection with deep neural nets. *Procedia Manufacturing*, *53*, 735-740.

Kazmi, M., Hafeez, B., Aftab, F., Shahid, J., & Qazi, S. A. (2023). A deep learning-based framework for visual inspection of plastic bottles. *IEEE Access*.

Kong, Y., & Ni, D. (2020). A semi-supervised and incremental modeling framework for wafer map classification. *IEEE Transactions on Semiconductor Manufacturing*, *33*(1), 62-71.

Koshti, A. M. (2018, March). Assessment of dye penetrant crack detectability in external corners using similarity analysis. In *Nondestructive Characterization and Monitoring of Advanced Materials, Aerospace, Civil Infrastructure, and Transportation XII* (Vol. 10599, pp. 322-331). SPIE.

Li, Z., Liu, F., Yang, W., Peng, S., & Zhou, J. (2021). A survey of convolutional neural networks: analysis, applications, and prospects. *IEEE transactions on neural networks and learning systems*, *33*(12), 6999-7019.

Loukil, Z., Mirza, Q. K. A., Sayers, W., & Awan, I. (2023). A deep learning based scalable and adaptive feature extraction framework for medical images. *Information Systems Frontiers*, 1-27.

Obaid, T., Abu-Naser, S. S., Abumandil, M. S., Mahmoud, A. Y., & Ali, A. A. A. (2022, November). Age and Gender Classification from Retinal Fundus Using Deep Learning. In *The International Conference of Advanced Computing and Informatics* (pp. 171-180). Cham: Springer International Publishing.

Rodríguez-Gonzálvez, P., Rodríguez-Martín, M., Ramos, L. F., & González-Aguilera, D. (2017). 3D reconstruction methods and quality assessment for visual inspection of welds. *Automation in construction*, *79*, 49-58.

Sethy, P. K., Behera, S. K., Ratha, P. K., & Biswas, P. (2020). Detection of Coronavirus Disease (COVID-19) based on Deep Features and Support Vector Machine. *International Journal of Mathematical, Engineering and Management Science*. *Vol. 5, No. 4,* 643-651.

Sharma, N., Sharma, R., & Jindal, N. (2021). Machine learning and deep learning applications-a vision. *Global Transitions Proceedings*, *2*(1), 24-28.

Shipway, N. J. (2019). *Automated defect detection for fluorescent penetrant inspection using machine learning* (Doctoral dissertation, Imperial College London). https://www.imperial.ac.uk/

Shipway, N. J., Huthwaite, P., Lowe, M. J. S., & Barden, T. J. (2021). Using ResNets to perform automated defect detection for Fluorescent Penetrant Inspection. *NDT & E International*, *119*,

Tercan, H., & Meisen, T. (2022). Machine learning and deep learning based predictive quality in manufacturing: a systematic review. *Journal of Intelligent Manufacturing*, *33*(7), 1879-1905.

Wang, J., Khan, M. A., Wang, S., & Zhang, Y. (2023). SNSVM: SqueezeNet-guided SVM for breast cancer diagnosis. *Computers, materials & continua*, *76*(2), 2201.

Xu, J., Kovatsch, M., Mattern, D., Mazza, F., Harasic, M., Paschke, A., & Lucia, S. (2022). A review on AI for smart manufacturing: Deep learning challenges and solutions. *Applied Sciences*, *12*(16), 8239.

Xu, C., Wei, G., Guan, Y., Zhang, S., Wang, H., Chen, X., ... & Liu, H. (2024). High-performance deep learning segmentation for non-destructive testing of X-ray tomography. *Journal of Manufacturing Processes*, *128*, 98-110.

Yang, L., Wang, H., Huo, B., Li, F., & Liu, Y. (2021). An automatic welding defect location algorithm based on deep learning. *Ndt & E International*, *120*, 102435.

Yu, L., Yang, E., Luo, C., & Ren, P. (2023). AMCD: an accurate deep learning-based metallic corrosion detector for MAV-based real-time visual inspection. *Journal of Ambient Intelligence and Humanized Computing*, *14*(7), 8087-8098.